Study of an Axial Injection Torch

K. Gadonna[1*], O. Leroy[1], L.L. Alves[2], C. Boisse-Laporte[1] and P. Leprince[1]
[1]Laboratoire de Physique des Gaz et des Plasmas, UMR CNRS/UPS 8578, Orsay, France
[2]Instituto de Plasmas e Fusão Nuclear, Laboratório Associado, IST, Lisboa Portugal
*katell.gadonna@u-psud.fr

Abstract: The axial injection torch (TIA for "Torche à Injection Axiale" in french) [1] produces high-density plasmas (~ a few cm length and a few mm radius) by coupling a flowing gas (a few L/min at atmospheric pressure) to microwave power (500-900 W) at 2.45 GHz frequency. Our study is about both the experimental characterization and the modeling of a TIA operating in helium, to understand the distribution of its electromagnetic field, the flow of the gas/plasma system, and the plasma-to-gas heat transfer. Experiments have a double purpose: to obtain input data for the model and to validate its results. The aim of the modeling is to describe the gas/plasma system in terms of its density, velocity and energy, by coupling three calculation modules: (i) electromagnetic, which solves Maxwell's equations considering the permittivity of the different media; (ii) hydrodynamic, which solves the Navier-Stokes' equations for the gas/plasma system; and (iii) plasma, still under development, which solves the fluid-type equations for the plasma electrons and ions.

Keywords: microwave plasmas, atmospheric pressure, modeling

1. Introduction

Among the different types of microwave plasma torches, the axial injection torch (TIA) [1] has been used for several years to create chemically active species, in applications such as gas analysis, surface processing, and gaseous waste treatments [2]. Here, we intend a different kind of application, aiming the volumetric heating of gas (e.g. helium). Our study is about both the experimental characterization and the modeling of a TIA, to understand the distribution of its electromagnetic field, the flow of the gas / plasma system, and the heat transfer from the plasma to the gas.

Experiments have a double purpose: to obtain input data for the model and to validate its results. Modeling describes the gas / plasma system, produced within a dielectric tube, in terms of its density, velocity and energy, by coupling three calculation modules:
- electromagnetic (EM-3D), which solves Maxwell's equations considering the permittivity of the different media;
- hydrodynamic (HD-2D), which solves the Navier-Stokes' equations for the gas / plasma system, including the gas thermal energy balance equation;
- plasma (P-1D), which solves the fluid-type equations for the plasma electrons and ions.

The electromagnetic and the hydrodynamic features of this problem have been analyzed in previous works, for a closed reactor configuration [3]. Here, we have developed the EM and the ED modules by using the commercial software COMSOL Multiphysics® [4].

2. Experimental Results

Figure 1 presents a schematics of the experimental set-up used here. The configuration in study consists of a dielectric tube (~40 cm length and ~5 cm in diameter) coupled to the TIA's nozzle (2 mm in diameter). Helium is injected at atmospheric pressure into the TIA (with flow rates of a few L/min), producing a high luminosity, high density plasma [5] (~3 cm length and 1 mm radius) at the nozzle's exit, generated by coupling of microwave power (500-900 W) at 2.45 GHz frequency.

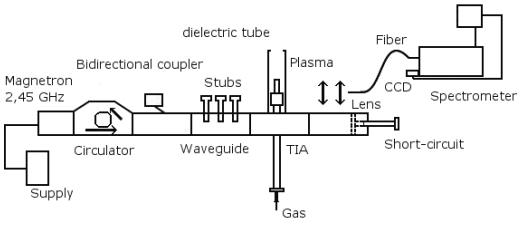

Figure 1. Schematic representation of the experimental set-up.

A thermal probe is used to measure the temperature of the tube wall, whose profile is adopted as boundary condition to the

hydrodynamic module. Optical emission spectroscopy diagnostics allow to obtain the electron density and temperature (by measuring the Stark broadening of the H_α and H_β atomic lines), and the gas temperature (by fitting the ro-vibrational spectra emitted by the second positive system of N_2, using the SPECAIR software [6]), at various positions along the plasma axis (top, middle and bottom).

In the simulations, the plasma is assumed to begin 1 mm up from the nozzle's end, and is defined by imposing its electron density n_e and temperature T_e (see profiles on Figure 2). Typical experimental values are $n_{eMAX} \sim 5\text{x}10^{14}$ cm^{-3}, $T_{eMAX} \sim 2\text{x}10^4$ K and $T_g \sim 3\text{x}10^3$ K for the gas temperature (in fact, T_g varies from 3200 to 2800 K between the bottom and the top of the plasma).

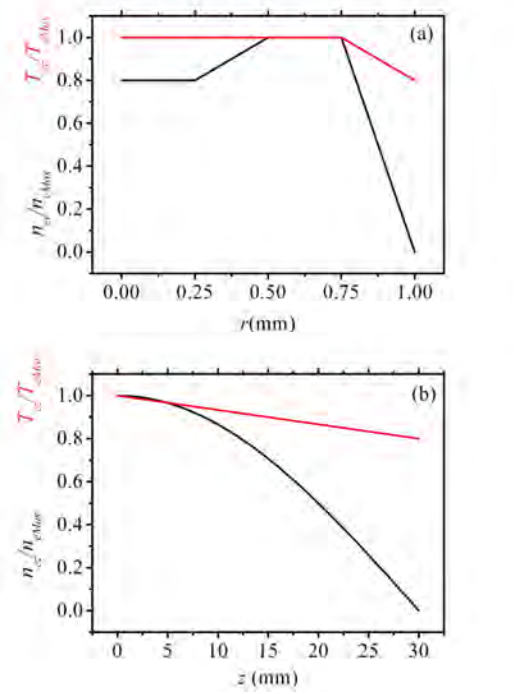

Figure 2. Radial (a) and axial (b) profiles of the plasma electron density (curves in black) and temperature (red) adopted in simulations.

3. Electromagnetic Module

3.1 Maxwell's Equations

The distribution of the electromagnetic field in the presence of plasma is calculated by solving the equation for the electric field $\vec{E}$, derived from the laws of Maxwell-Ampere and Faraday

$$\vec{\nabla}\cdot\left(\frac{1}{\mu_r}\vec{\nabla}\times\vec{E}\right)-k_0^2\left(\varepsilon_r-\frac{j\sigma}{\omega\varepsilon_0}\right)\vec{E}=\vec{0} \quad (1)$$

where ε_r and μ_r are the relative permittivity and permeability, respectively, of the different media (vacuum and plasma); ε_0 is the permeability of vacuum; σ is the (plasma) conductivity; and $k_0=\omega\sqrt{\varepsilon_0\mu_0}$ is the wave-number in vacuum. For plasma:

$$\varepsilon_r=1-\frac{\omega_p^2}{\omega^2\left(1-\frac{j\nu}{\omega}\right)}$$

$$\sigma=\frac{n_e e^2}{m_e(\nu+j\omega)}$$

$$\mu_r=1$$

with $\omega=2\pi\nu_{HF}$ (ν_{HF} = 2.45 GHz) the microwave excitation frequency, $\omega_p=\sqrt{n_e e^2/m_e\varepsilon_0}$ the plasma frequency (e and m_e are the electron charge and mass, respectively), and ν the electron-neutral collision frequency.

To propagate microwaves in a medium, its permittivity must be positive. For plasma, this implies that its frequency must be lower than the excitation frequency, which yields a critical (minimum) electron density (at 2.45 GHz) of

$$n_c=\frac{\varepsilon_0 m_e\omega^2}{e^2}=7.4\times10^{10} \text{ cm}^{-3}.$$

3.2 Numerical Model

The EM module uses the "rwf" mode from the Radio Frequency module of COMSOL Multiphysics®, which is solved in 3D at 2.45 GHz. Figure 3 represents the computational domain adopted, where equation (1) is discretized using a 3D triangular mesh.

The boundary conditions for the waveguide and the torch correspond to those of a perfect electric conductor, except for the input plane (P.E.) where the microwave power is supplied. At this boundary, a port condition for a rectangular mode TE_{10} is imposed. Moreover, this configuration is surrounded by typical PML Cartesian-type regions, where scattering boundary conditions were assumed**.**

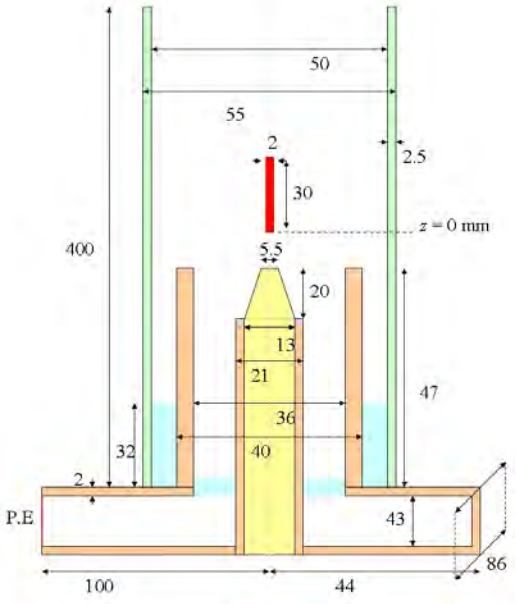

Figure 3. Transversal section of the 3D computational domain adopted to solve the EM module, showing the waveguides (in brown), the torch (yellow), the dielectric tube (green), the Teflon (blue) and the plasma (red). All dimensions are in millimeters and the diagram is not in scale. The plasma is located 1 mm up from the nozzle's end.

The numerical solution uses the solver PARDISO and adopts a convergence criterion that imposes relative errors, between consecutive calculations, smaller than 10^{-6}.

3.3 Results and Discussion

Figure 4 shows the axial profile of the modulus of the electric field components in the plasma, calculated for input microwave power of 700 W and different maximum electron densities.

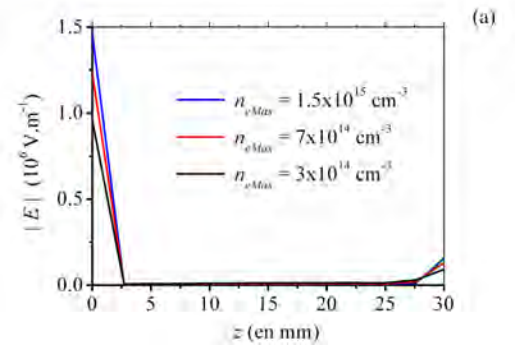

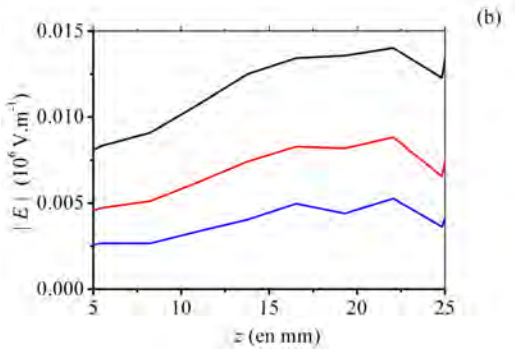

Figure 4. (a) Axial profile (at $r = 0$) of the modulus of the electric field components in the plasma (at 700 W input power), calculated for the following maximum electron densities (in 10^{14} cm^{-3}): 3 (curve in black), 7 (red) and 15 (blue). (b) is just a zoom of (a) between 5 and 25 mm.

Although the plasma is expected to behave like a conductor, we observe that the microwave field is able to penetrate slightly into the plasma region [see Figure 4(a) near z=0], and that this effect is enhanced with an increase in the electron density. However, as n_e increases (inducing an increase also in the plasma conductivity), the electron field decreases inside the plasma [see Figure 4(b)].

4. Hydrodynamic Module

4.1 Navier-Stokes' Equations

The distribution of mass density ρ, flow $\rho\vec{v}$ and temperature T_g of the neutral gas particles, in the presence of a plasma heating source, is calculated by solving the corresponding mass, momentum, and thermal energy balance equations for helium

$$\vec{\nabla}\cdot(\rho\vec{v}) = 0 \quad (2)$$

$$\rho(\vec{v}\cdot\vec{\nabla})\vec{v} = -\vec{\nabla}p - \vec{\nabla}\cdot\vec{\tau} + en_i\vec{E}_{dc} \quad (3)$$

$$\rho C_v\left(\vec{v}\cdot\vec{\nabla}\right)T_g - \vec{\nabla}\cdot\left(\lambda_g\vec{\nabla}T_g\right) + p\vec{\nabla}\cdot\vec{v} = 3\frac{m_e}{M_g}n_e\nu k_B\left(T_e - T_g\right) + e\vec{\Gamma}_i\cdot\vec{E}_{dc} \quad (4)$$

where $p = \left(\rho/M_g\right)k_BT_g$ is the gas pressure (with M_g the mass of a gas atom and k_B the Boltzmann's constant), $\vec{\tau}$ is the viscosity tensor given by

$$\vec{\tau} = -\eta\left[\vec{\nabla}\vec{v} + (\vec{\nabla}\vec{v})^T - (2/3)\vec{\nabla}.\vec{v}\vec{I}\right]$$

(with η the viscosity coefficient), C_v is the gas heat capacity at constant volume, λ_g is the gas thermal conductivity, $\vec{E}_{dc}$ is the space-charge field, and n_i and Γ_i are the ion density and flux, respectively. Since the discharge runs at atmospheric pressure, we assume ambipolar conditions for the ion parameters and the space-charge field (namely by imposing the quasi-neutrality n_i=n_e), when writing the ion terms $en_i\vec{E}_{dc}$ and $e\vec{\Gamma}_i \cdot \vec{E}_{dc}$.

Notice the introduction, in equation (4), of several supplementary terms (with respect to the *standard* energy balance equation of a flowing gas), accounting for the various channels of energy exchange between the plasma and the gas. In particular, the terms on the left-hand side of this equation correspond to convection, conduction and the work of pressure forces, whereas the terms on its right-hand side correspond to electron-neutral elastic collisions and ion drift under the action of the space-charge field.

4.2 Numerical Model

Equations (2) to (4) are solved for an input gas flow of 7 L min^{-1}, i.e. for an average input gas velocity of 35 m s^{-1}. For these conditions, the Mach number and the Reynolds' number are small (M<0.3 and Re<2000), indicating that the flow is subsonic and non-turbulent.

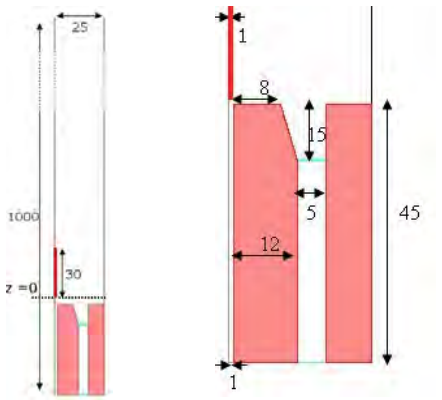

Figure 5. Axis-symmetric 2D computational domain adopted to solve the HD module (a) and zoom of this arrangement at the nozzle's exit (b). All dimensions are in millimeters and the diagram is not in scale. The plasma is located 1 mm up from the nozzle's end.

The HD module uses the the "spf" and "ht" modes from the Fluid Flow and the Heat Transfer modules of COMSOL Multiphysics®, which are solved within the axis-symmetric 2D computational domain (including the torch, the dielectric tube and the plasma) represented in Figure 5. Meshing is performed automatically by the software and includes triangular features.

The boundary conditions are the following. At the axis (r=0) we impose axis-symmetry conditions. At the walls, we impose $\vec{v}=0$ (corresponding to a no-slip condition) and the gas temperature. At the input opening (z=0), the gas velocity is prescribed according to

$$v(r) = 2v_0\left(1-\frac{r^2}{R^2}\right)$$

where v_0 is the average input gas velocity and R=1 mm is the nozzle's radius. At the output opening, we set the pressure as p=p_{atm}.

The numerical solution uses the solver PARDISO and adopts a convergence criterion that imposes relative errors, between consecutive calculations, smaller than 10^{-6}.

4.3 Results and Discussion

Figure 6 presents the axial profile of the gas temperature within the plasma region for different maximum electron temperatures, calculated with and without the ion terms in equations (3) and (4).

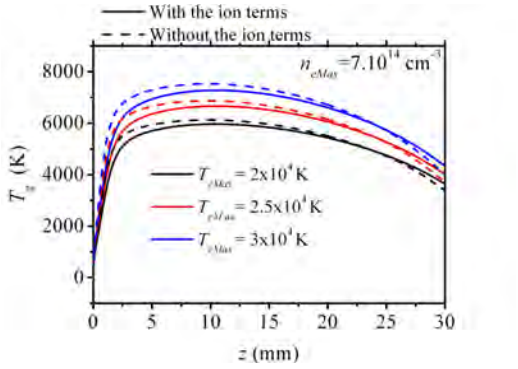

Figure 6. Axial profile (at r = 0) of the gas temperature within the plasma region (at 7 L min^{-1} input gas flow), calculated with (solid curves) and without (dashed) ions terms, for n_{eMAX} = 7x10^{14} cm^{-3} and the following maximum electron temperatures (in 10^4 K): 2 (curve in black), 2.5 (red) and 3 (blue).

We observe that the gas temperature value is sensitive to variations in the electron temperature and that its profile is affected by the inclusion of the ion drift terms in the hydrodynamic equations. Both results confirm the existence of an efficient plasma-to-gas power transfer. The gas temperatures predicted by simulations (at r=0) are found above those observed experimentally. However, one must note that measurements are in fact the result of a radial averaging (performed at a given z position), and that the gas temperature decreases along the radius.

For the same conditions as before, figure 7 shows the axial profile of the modulus of the gas velocity within the plasma region.

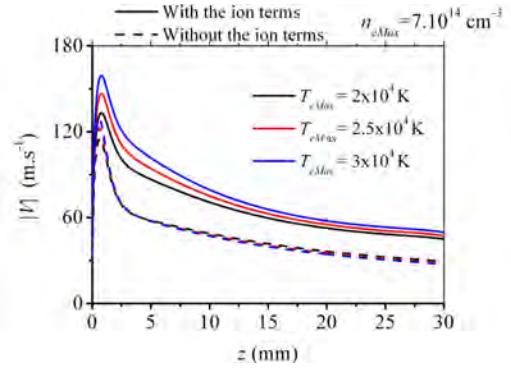

Figure 7. Axial profile (r = 0) of the modulus of the gas velocity within the plasma region, for the same conditions as in Figure 6.

The results in this figure reveal that (i) the plasma changes the path of the gas flow, and (ii) the introduction of the ion terms (associated to their drift within the space-charge sheath) enhances the gas flow velocity.

Figures 8 and 9 plot the axial profiles of the gas temperature and of the modulus of the gas velocity, within the plasma region, for different maximum electron densities, calculated with and without the ion terms in equations (3) and (4). Once again, the results in these figures confirm the efficient plasma-to-gas power transfer and the influence of the ion terms on both the gas temperature profile and the gas flow velocity.

Numerical tests show that the profile of the gas temperature is affected also by the input gas flow. An increase in the flow leads to longer relaxation lengths in the axial direction for the gas temperature, accompanied by a decrease in its peak (in plasma region) and an increase in its tail. The effect is similar to that observed in Figures 6-7 and 8-9, due to an increase in the gas velocity associated with the introduction of the ion terms.

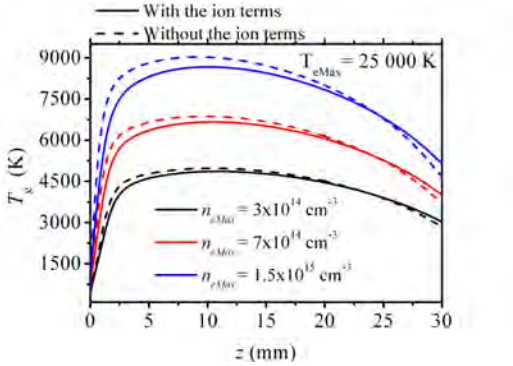

Figure 8. Axial profile (at r = 0) of the gas temperature within the plasma region (at 7 L min^{-1} input gas flow), calculated with (solid curves) and without (dashed) ions terms, for T_{eMAX} = 2.5x10^4 cm^{-3} and the following maximum electron densities (in 10^{14} cm^{-3}): 3 (curve in black), 7 (red) and 1.5 (blue).

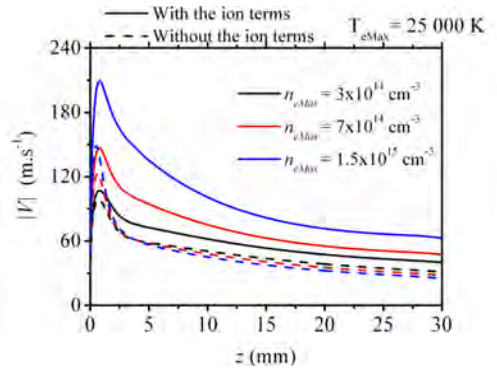

Figure 9. Axial profile (r = 0) of the modulus of the gas velocity within the plasma region, for the same conditions as in Figure 8.

5. Conclusions

The development of two calculation modules [electromagnetic (EM) and hydrodynamic (HD)] using COMSOL Multiphysics® has allowed describing the influence of a plasma, created by an axial injection torch, on the electromagnetic excitation field of the device and on the gas flow velocity and temperature distributions.

The EM results showed that the electromagnetic field exhibits a maximum value in the plasma region near the nozzle's tip and that its axial component is able to penetrate the plasma.

The main HD results are the following: (i) the plasma changes the path of gas flow; (ii) there is an efficient plasma-to-gas power transfer, demonstrated by the influence of the plasma energy-density on the gas temperature; (iii) the introduction in the hydrodynamic equations of ion terms (associated to their drift within the space-charge sheath) enhances the gas flow velocity and modifies the gas temperature profile.

Work is in progress to develop a plasma (P) module, describing the plasma in terms of charged particles transport along the z direction. The P module will use the results obtained with the other calculation modules, providing self-consistent information about the plasma to be used as EM and HD input data.

6. References

1. M. Moisan, G. Sauvé, Z. Zakrzewski, J. Hubert, An atmospheric pressure waveguide-fed microwave plasma torch: the TIA design, *Plasma Sources Sci. Technol.*, **3**, 584 (1994)

2. C. Tendero, C. Tixier, P. Tristant, J. Desmaison, P. Leprince, Atmospheric pressure plasmas: A review, *Spectrochimica Acta B*, **61**, 2 (2006)

3. L.L. Alves, R. Alvarez, L. Marques, J. Rubio, A. Rodero, M.C. Quintero, Modeling of an axial injection torch, *Eur. Phys. J. Appl. Phys.*, **46**, 21001 (2009)

4. http://www.comsol.com/

5. A. Ricard, L. St-Onge, H. Malvos, A. Gicquel, J. Hubert, M. Moisan, Torche à plasma à excitation micro-onde: deux configurations complémentaires, *J. Phys III,* **5**, 1269 (1995)

6. http://www.specair-radiation.net/

8. Acknowledgements

L.L. Alves was supported by the Portuguese Foundation for Science and Technology (Project PTDC/FIS/65924/2006).